Case Studies in Construction Materials 22 (2025) e04319

Contents lists available at ScienceDirect

Case Studies in Construction Materials

journal homepage: www.elsevier.com/locate/cscm

Preliminary characterization and evaluation of local concrete sludges for use as supplementary cementitious materials

Ashfaque Ahmed Jhatial [a,*], Iveta Nováková [a], Eirik Gjerløw [a], Christian John Engelsen [b]

[a] Department of Building, Energy and Material Technology, The Arctic University of Norway, Lodve Langes gata 2, Narvik 8514, Norway
[b] SINTEF Community, Department of Building and Infrastructure, Blindern, P.O. Box 124, Oslo NO-0314, Norway

ARTICLE INFO

Keywords:
Supplementary Cementitious Materials (SCMs)
Industrial waste
Concrete Sludge
Material Characterization
Chemical Composition
Particle Size
Mineralogy

ABSTRACT

Concrete sludge (CS) is an emerging supplementary cementitious material (SCMs). However, the diverse range of SCMs and their various sources for each necessitate initial characterization and evaluate the potential of CS as a SCM. In this study, CS were collected from seven different concrete producers (designated as CS1 to CS7) in the Northern Norway region. This preliminary characterization aims to provide valuable insights into the feasibility of using CS in cement or concrete production. It was determined that the chemical composition of CS was found to meet the EN 450–1 requirements, while most of the CS evaluated, exhibited hydraulic characteristics. The Rankin Classification of analyzed CS indicates a prevalent hydraulic nature, with most CS exhibiting CaO/SiO_2 ratios greater than 2.0, thus suggesting potential for hydraulic applications. It was also observed that with 30 minutes of pulverizing, the particle size of the CS samples exhibited an average decrease ranging from 6.8 % to 78 %. This variation is likely due to differences in initial particle size and composition. Larger particles are generally more susceptible to breakdown during pulverization, which explains the higher reduction observed in some samples. Conversely, samples with higher coarse sand content and the resistance of specific aggregates to grinding exhibited the smallest reduction. These differences highlight the impact of material composition on the effectiveness of the pulverization process. An increase in the specific surface area and a decrease in the particle size of CS were observed after grinding, showing the potential for mechanical activation of CS as a potential SCM. However, prolonged pulverization beyond 30 minutes is not recommended, as only marginal improvement beyond 30 minutes of pulverization were observed. The XRD analysis revealed that the CS samples contained 2.29–28.47 %, with an average of 8.3 % amorphous content, reflecting the variation of cement paste in the CS. The findings suggest that CS can be categorized into two SCMs based on their operation: precast CS, characterized by siliceous and alkali-rich properties, and ready-mix CS, which is lime-rich and exhibits hydraulic properties, enabling tailored applications in cement and concrete production.

* Corresponding author.
E-mail addresses: ashfaque.a.jhatial@uit.no (A.A. Jhatial), iveta.novakova@uit.no (I. Nováková), eirik.gjerlow@uit.no (E. Gjerløw), christianjohn.engelsen@sintef.no (C.J. Engelsen).

https://doi.org/10.1016/j.cscm.2025.e04319
Received 4 July 2024; Received in revised form 13 December 2024; Accepted 26 January 2025
Available online 31 January 2025

1. Introduction

The construction industry, often regarded as the backbone of modern infrastructure and urban development, has brought tremendous progress and enhanced comfort in societies worldwide. However, this progress has come at a significant environmental cost. The production of cement, a key ingredient in concrete, accounts for one of the most significant carbon footprints in the construction industry. Calcination—the process of heating limestone (calcium carbonate) to high temperatures—and the use of fossil fuels release carbon dioxide (CO_2) during cement clinker production [1]. The CO_2 gas is a significant greenhouse gas contributing to global warming. While the natural greenhouse effect maintains Earth's temperature by trapping solar heat, the human activities such as the industrial processes and fossil fuel combustion have considerably elevated the global greenhouse gases levels, subsequently contributing to climate change. Reports [2] have estimated that approximately 5–8 % of the total global CO_2 gas emissions are emitted by the cement industry alone.

The impact of such CO_2 gas emissions is being felt worldwide through climate change and global warming, and since the cement industry is one of the leading emitters, the building industry's greenhouse gas emissions have come under scrutiny. These environmental concerns have forced the industry into a fundamental shift in concrete production, with the use of Supplementary Cementitious Materials (SCMs) as a crucial technology for reducing concrete production's environmental impact while maintaining the structural integrity and functionality of the concrete [3,4].

The use of SCMs as a partial substitute for cement content in producing eco-friendly low carbon concrete plays a critical role in diminishing the reliance on cement, mitigating the depletion of natural resources, and reducing the carbon footprint associated with this vital construction waste by-product [5]. The SCMs, which are primarily derived from by-products or waste materials, help limit the emission of CO_2. The remaining CO_2 footprint comes mainly from their transportation, preparation, and treatment to enhance reactivity [3]. These generated emissions are comparatively lower than those stemming from cement production, sometimes the CO_2 emissions could even be negligible. The utilization of SCMs in the concrete gives two major benefits; first, by partially substituting cement, it allows the reduced dependence of cement and second, it contributes to waste management as the industrial wastes are being reused [6].

With the concrete industry becoming more open to the utilization of SCMs, it now faces a significant challenge with the supply of available SCMs, as the existing SCMs can only meet approximately 15 % of its overall demand. Fly ash, a byproduct of pulverized coal combustion in power plants, has traditionally been the dominant SCM; however, its availability is diminishing due to the phasing out of coal-fired power plants and the transition to renewable energy sources. Additionally, most of the available ground granulated blast furnace slag is already being used to its capacity in cement production, however, its supply is decreasing due to increased steel recycling and direct iron reduction. Silica fume, while effective, is costly, potentially inflating production expenses when used as a cement substitute. Furthermore, existing SCMs are not uniformly produced or accessible in all regions, necessitating long-distance transportation and contributing to elevated CO_2 emissions and costs. As the industry rapidly evolves and international trade of SCMs grows, exploring new SCM sources becomes imperative. One promising emerging SCM is Concrete Sludge.

Concrete sludge (CS) or concrete slurry, is a waste stream generated during concrete production at ready-mix or precast concrete facilities [7]. In this process, the wastewater from cleaning ready-mix trucks and batching plants is directed to sedimentation tanks where fine materials are allowed to settle [8]. These remaining fine materials are recognized as CS.

While it is challenging to quantify the global production of CS precisely, researchers have made efforts to provide a rough estimate. Based on the total global cement production of 4 billion metric tons [9], an approximate estimation suggests that CS generated stands at roughly 260 million metric tons [10]. Given that cement constitutes around 14 % of the mass in 1 m^3 of concrete, the generated CS represents approximately 0.9 % of the total concrete mass produced globally, assuming an overall concrete production of 28 billion metric tons. In Europe, fresh concrete waste generated during manufacturing or because of truck cleaning and washing is estimated to range from 1 % to 4 % of the total concrete production [11]. The CS is generally consisting of a combination of the finest aggregates and hydrated/carbonated residuals of cement [7]. Given the substantial generation of CS, researchers are exploring its potential as a SCM. Understanding the fundamental material properties of new SCMs before large-scale testing is essential. This characterization helps predict and control their behaviour in concrete mixtures, including effects on setting time, strength development, and durability. Table 1 summarizes the common SCM characterization techniques, covering their chemical composition, phase composition, and

Table 1
Common SCM characterization techniques [12].

Technique	Information	Assets
Laser Diffractometry	PSD – size range 0.1–1000 μm	Standard, rapid, reproducible measurement
He Pycnometry	Density	Common, rapid, reproducible, straightforward
BET N_2 Sorption	Specific surface area, size, and shape of pores	Common, includes internal porosity
X-Ray Fluorescence Spectrometry (XRF)	Element composition	Rapid, straightforward, accurate
Thermogravimetric Analysis (TGA)	Detection of phases and changes based on thermal exposure	Accessible, straightforward, quantitative
X-Ray Diffraction (XRD)	Crystalline phase composition	Accessible, rapid, multiple-phase identification and quantification
Scanning Electron Microscopy (SEM)	Spatially resolved phase information (size, shape, texture, distribution, and microstructure)	It can be combined with microchemical analysis.

physical characteristics such as particle size distribution (PSD), density, and specific surface area.

Although there are many established methods and techniques to characterize any SCM, as mentioned in Table 1, this study will be limited to four commonly used techniques to determine CS characteristics, including;

(1) *Particle density and a laser diffraction analyzer* are used to determine the PSD, indicating the range of particle sizes and specific surface area.
(2) *XRF* is used to determine the chemical/oxide composition of CS to explore whether they potentially are latent hydraulic or pozzolanic nature. Pozzolanic SCMs are classified according to ASTM C618 [13] or Rankin classification based on the CaO/SiO_2 ratio: < 0.5 is pozzolanic, 1–1.5 is latent hydraulic, and > 2 is hydraulic.
(3) *XRD* analysis is used for qualitative and quantitative mineral composition analysis.
(4) *SEM with Energy Dispersive Spectroscopy (EDS)*, to analysis the microstructure and elemental composition of CS.

This study is significant because it applies the existing non-destructive test methods to systematically assess the potential of CS as SCMs. Detailed characterization is crucial for evaluating the suitability of any SCM, in this case CS, for concrete applications. It ensures that the utilization of CS as SCMs reduces the waste, ultimately contributing to a more sustainable and reliable construction industry.

2. Materials and methods

2.1. Collection and preparation of raw materials

The raw CS samples for characterization were collected from seven different concrete plants in Northern Norway. These plants utilize CEM I 52,5 R, CEM II/B-M(V-L) 42,5 R, and low calcareous coal fly ash from Heidelberg Materials Sement Norge and silica fume were binder materials while Dynamon 23 with 18 % solids and Mapeair SA produced by Mapei, were used as superplasticizer and air-entraining admixture, respectively. However, the choice of aggregates varied depending on each plant́s location. The CS1 to CS6 were collected from concrete plants with various operations, as detailed in Table 2, while CS7, stored for two years, was assessed for property changes. The CS4, CS5, CS6 and CS7 were within the same vicinity and used the same aggregates.

The CS was collected in a wet state and oven-dried at 50 °C to prevent unwanted chemical reactions. After drying, the CS were sieved using a 2 mm sieve to remove large particles, steel fibres and other impurities that the collected samples may contain. This material is referred to as P0 (unpulverized sample). Furthermore, a 1.5 kg portion of each sample material was subjected to pulverization using a ball mill with 3 liters of porcelain drums and grinding medium at a speed of 400 rpm for two specific durations, 30 min and 60 min (P30 and P60, respectively). The pulverization of CS eliminates lumps caused by the drying process. In total, 21 samples were prepared for characterization, as shown in Table 2.

Table 2
Overview of material origin, designation and pulverization time.

Source				Pulverization duration (min)	Designation
	Precast		Ready-mix		
	Hollow-core slabs/sawing	Sawing elements			
CS1	X			0	CS1P0
				30	CS1P30
				60	CS1P60
CS2	X	X	X	0	CS2P0
				30	CS2P30
				60	CS2P60
CS3		X		0	CS3P0
				30	CS3P30
				60	CS3P60
CS4			X	0	CS43P0
				30	CS4P30
				60	CS4P60
CS5			X	0	CS5P0
				30	CS5P30
				60	CS5P60
CS6			X	0	CS6P0
				30	CS6P30
				60	CS6P60
CS7		X		0	CS7P0
				30	CS7P30
				60	CS7P60

Note: CS = concrete sludge, P = pulverization

2.2. Characterization methods

Processed CS materials were characterized in the concrete laboratory at UiT, the Arctic University of Norway, in Narvik. The characterization focused on three primary parameters: chemical composition, PSD, and mineralogical composition.

The handheld XRF, Hitachi X-MET8000 Expert Geo, with a Mining Light Element preset, was used to determine the chemical composition of the different materials. A portable XRF device offers rapid sample analysis but has limitations in detecting elements with atomic numbers lower than magnesium. Since the XRF determines the elements, conversion from element mass percentage to oxide mass percentage was done to express them as oxides [14]. The chemical composition of potential SCMs is compared with the requirements of ASTM C618 [13] to see if CS is chemically suitable for pozzolanic or latent hydraulic reaction. While Rankińs classification was used to evaluate the CaO/SiO_2 ratio to infer the reactivity and type of cementitious behavior, such that $CaO/SiO_2 < 0.5$ indicative of pozzolanic behavior, $CaO/SiO_2 = 1 - 1.5$ indicates latent hydraulic behavior and $CaO/SiO_2 > 2$ indicative of hydraulic behavior. Both ASTM C618 [13] and Rankin classifications are indirect methods for pozzolanicity which rely on chemical composition (e.g., silica, alumina, and calcium content).

The densities were determined using a water pycnometer according to the EN 1097–7 [15]. The Malvern Panalytical Mastersizer 3000 instrument was used to determine the PSD and the specific surface area using the wet cell procedure, which involves dispersing the particle in the dispersant.

The PSD and fineness of SCM significantly influence the properties of concrete. PSD obtained through laser diffraction is a quick and easy method. However, multiple authors have emphasized the selected refractive index's significant impact on PSD measurements' outcomes using Laser Diffraction techniques. This influence is closely tied to the fundamental principle of laser diffractometry, where scattering occurs due to disparities in the refractive index between the particle being measured and the medium in which it is suspended. In cases where there is a lack of information regarding the sample's optical properties, researchers adjust refractive indices ('n' and 'k') and optimize results. As for this current experimental work, the n and k values of cement from the Malvern database were initially taken and then further optimized using the optical property optimizer feature within the Malvern Mastersizer 3000.

The XRD determined the crystalline phase compositions of the CS in a Malvern Panalytical Aeris Minerals Edition X-ray diffractometer equipped with CuKα radiation with λ= 1.54060 Å, a secondary graphite monochromator and a proportional counter. Data were collected at 40 kV and a current of 15 mA, over the 2θ range from 4 to 80° at a scan rate of 1.2° 2θ/min. All Rietveld refinements with pseudo-Voigt function and a polynomial background were performed using the X'Pert HighScore Plus diffraction software from Panalytical with PDF4 + (2023) powder diffraction files. The internal standard method [16] used calcium fluoride to determine the amorphous content.

Additionally, the microstructural and elemental analysis was conducted using SEM-EDS on the Hitachi TM 3030 Benchtop SEM, at UiT Tromsǿs Department of Geology, UiT Tromsø. This SEM-EDS technique provides high-resolution imaging and elemental composition data of CS particles, allowing for detailed characterization of particle size, shape, and surface morphology on microscopic level, as well as the identification of dominant elements such as Ca, Si, and minor components.

Table 3
Chemical Composition of CS (given in weight %).

Material	SiO_2	Al_2O_3	Fe_2O_3	CaO	K_2O	P_2O_5	MgO	SO_3
CS1P0	14.2	2.8	15.1	53.3	2.8	0.2	0.8	0.7
CS1P30	15.2	2.9	15.4	53.3	2.9	0.2	0.6	0.6
CS1P60	15.6	4.6	15.1	50.3	5.8	0.2	0.0	0.1
CS2P0	13.2	2.1	14.6	55.3	2.7	0.2	0.9	0.9
CS2P30	14.0	2.6	15.3	54.0	2.3	0.2	0.9	0.8
CS2P60	12.4	2.0	16.7	56.7	1.9	0.2	0.8	0.7
CS3P0	27.3	4.1	17.0	35.8	6.1	0.2	0.0	0.7
CS3P30	23.8	3.5	17.3	38.6	6.2	0.2	0.0	0.6
CS3P60	24.1	4.6	18.5	35.1	6.2	0.2	1.3	0.5
CS4P0	8.5	3.4	14.4	62.3	1.5	0.1	0.0	0.7
CS4P30	11.0	3.0	13.2	61.1	1.4	0.1	1.0	1.0
CS4P60	12.0	2.9	13.0	60.4	1.4	0.1	0.9	1.0
CS5P0	15.5	2.7	11.2	56.8	2.8	0.2	0.0	2.6
CS5P30	14.0	2.4	11.2	58.1	2.7	0.2	0.4	2.0
CS5P60	16.6	3.1	10.9	55.0	3.0	0.2	0.4	2.1
CS6P0	14.1	2.1	15.9	53.4	3.8	0.2	0.5	1.3
CS6P30	14.5	2.5	17.6	51.1	3.4	0.1	0.4	1.4
CS6P60	15.5	3.2	16.5	50.4	3.3	0.3	0.4	1.4
CS7P0	28.3	5.0	19.6	28.2	8.7	0.3	0.2	0.0
CS7P30	32.2	5.4	17.2	27.1	8.3	0.3	0.0	0.2
CS7P60	34.1	5.4	16.0	26.5	8.3	0.3	0.1	0.2

3. Results and discussion

3.1. Chemical properties

3.1.1. Chemical composition analysis

The chemical composition of all materials, based on the XRF analysis, is presented in Table 3. The primary oxides detected were calcium oxide (CaO) and silicon oxide (SiO_2), while iron oxide (Fe_2O_3) was also present in considerable amounts. The presence of Fe may be attributed to various sources such as cement paste, natural aggregates and, to some extent, cutting of steel fibres and reinforced steel. Cumulative Fe_2O_3 content from different mineral sources from aggregates could likely contribute to the observed iron levels. It can be observed that with pulverization, the chemical composition has changed slightly. This could be attributed to 1) the mechanical pulverization process, which may amplify hardness disparities among various minerals or compounds, potentially producing finer particles from less resilient materials. This finer particulate matter can adhere to the harder surfaces of more complex particles, impeding their detection or reducing peak intensities in subsequent XRD or XRF analyses, and 2) slight changes in chemical composition could be due to contamination from the grinding medium, in the current study, porcelain drums and grinding medium were used [17].

The European standard EN 450–1 [18] provides guidelines for assessing fly ash suitability in concrete, which can also be applied to SCMs like CS. This standard specifies permissible levels for sodium oxide (Na_2O) equivalent, magnesium oxide (MgO), sulphur trioxide (SO_3), and phosphorus pentoxide (P_2O_5) to prevent adverse effects on concrete performance. However, compliance with these limits alone does not ensure the SCM's effectiveness or reactivity. Therefore, additional testing is required to evaluate the pozzolanic or hydraulic properties of the SCM and confirm its potential benefits in concrete.

The MgO reacts with water at a slower pace than CaO in the early stage, and due to this, excessive expansion may occur at a later stage, potentially leading to poor stability [19]. It also increases the volume due to $Mg(OH)_2$ formation. Higher MgO content has been reported to slightly reduce the compressive strength of concrete. Therefore, EN 450–1 [18] limits the MgO content of SCMs to 4 %. As shown in Table 3, all the CS had MgO content up to 1.3 %, which is significantly lower than the prescribed limit. The presence of P_2O_5 causes a reduction in strength, beyond 2.25 % content in clinker, cement fails to meet standard requirements. As shown in Table 3, the CS consisted of between 0.1 % and 0.3 %, well within the prescribed limit of $P_2O_5 \leq 5$ %.

As for the third limit, SO_3, EN 450–1 [18] has prescribed a 5 % limit; the CS recorded the SO_3 content between 0 % and 2.6 %. The importance of SO_3 in SCMs is that an increase in SO_3 content tends to accelerate the alite reactions (early strength gain) and cause the aluminate hydrate reaction to occur at a later stage. Interestingly, CS5 contained almost double the amount of SO_3 compared to other CS samples. CS3 and CS5 were collected from the same concrete plant, though CS3 was drilling sludge and CS5 was the sludge from washing concrete trucks. The difference in chemical composition between the two can be attributed to the washing sludge having a higher volume distribution of fine and medium sand particles. Fine aggregates can also be observed in the mineralogical composition discussed further.

3.1.2. Pozzolanic and hydraulic potential

According to ASTM C618 [13], any material can be classified as a pozzolanic material depending on the sum of pozzolanic oxides (SiO_2, Al_2O_3 and Fe_2O_3) as shown in Fig. 1. CS7 can be classified as Class C pozzolanic material since the sum of its pozzolanic oxides exceeds 50 %. However, it is important to note that the standard specifies the soluble reactive portion, and classification is solely based on element composition and may not accurately determine the pozzolanic behaviour of CS.

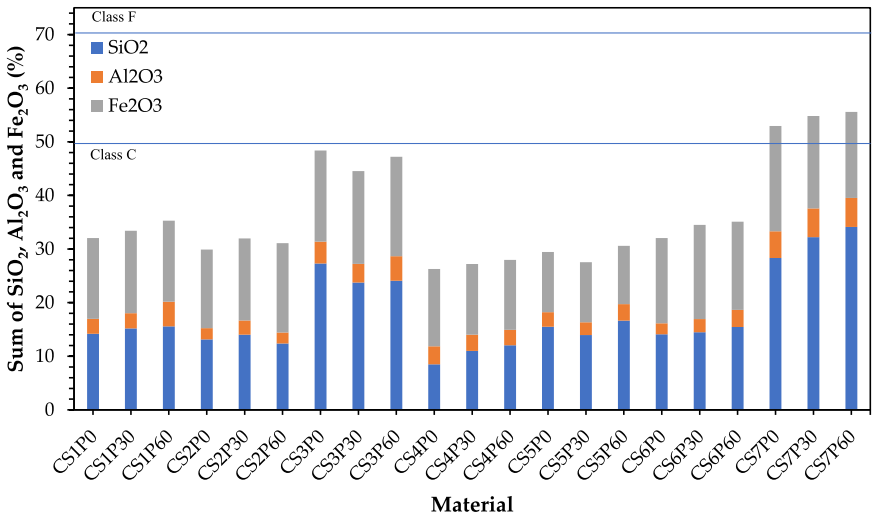

Fig. 1. Comparison of CS according to ASTM C618 [13].

CS4, collected from a different source, shows a chemical composition distinct from CS3 and CS7. Although it has lower Fe_2O_3 content (~14 %), these variations could influence its reactivity and potential pozzolanic behaviour. The Fe_2O_3 content may also be linked to the nature of the aggregate and collection methods. While CS4's results do not fully support the hypothesis that operations affect Fe_2O_3 content, they emphasize the importance of considering aggregate composition and chemical variability. This highlights the need for a comprehensive analysis to understand the impact of operations and materials on CS composition.

Based on the chemical composition comparison, CS7, which originated from the same source as CS3 but was kept in a closed environment for approximately 2 years, exhibited slight changes in elemental composition. Though these changes could potentially be caused by the ongoing hydration or carbonation processes during storage, as any unhydrated cement and other reactive components in CS7 could continue to hydrate in a closed environment, it is important to highlight that other factors may also contribute to the changes. Variation in raw material properties, production processes and/or potential analytical variability (such as the formation of new mineral phases affecting peak intensities), cannot be ruled out. The lack of baseline data on CS7 prior to storage limits the certainty of attributing these variations to storage-induced processes alone.

Additionally, CO_2 can cause carbonation, converting calcium hydroxide ($Ca(OH)_2$) into calcium carbonate. The changes observed in the elemental composition of CS7 might also be influenced by contamination with fines from the aggregates, which was not initially accounted for. This potential contamination should be considered when interpreting the results. These compositional changes suggest a continuing reactivity of the materials over time, which could affect their performance in various applications. Further studies are required to fully understand these implications.

Vaičiukynienė *et al.* [20] and Jadhav *et al.* [21] reported significant concentrations of CaO and SiO_2 in dry sludge using XRF analysis. Specifically, Vaičiukynienė *et al.* [20] found 47.1 % CaO and 25.9 % SiO_2, while Jadhav *et al.* [21] observed 40.9 % CaO and 14.9 % SiO_2. The chemical composition of the evaluated CS concurs with previous findings in the literature.

Another classification of SCMs to indicate which type of SCM the material can be is done by the Rankin classification [22]. It is a simple calculation based on the CaO/SiO_2 ratio. The Rankin classification of the analyzed materials underscores a prevalent hydraulic nature, with most exhibiting CaO/SiO_2 ratios within the hydraulic range. This consistency suggests a shared potential for hydraulic applications across the materials [20,21].

The readymix CS, i.e., CS4, CS5 and CS6, exhibited consistently hydraulic properties, with their CaO/SiO_2 ratios ranging between 7.33 and 5.03. In contrast, the precast CS, i.e., CS1, CS2 and CS3, exhibited varying degree of hydraulicity. The CS1 and CS2 exhibited CaO/SiO_2 ratios between 3.22 and 4.57, indicating high lime content and reactivity, while CS3 with CaO/SiO_2 ratio between 1.31 and 1.46, falls within the latent hydraulic material category.

The CaO/SiO_2 ratio of unpulverized CS7 (CS7P0) was 1.00, while the pulverization of CS7 further decreased the CaO/SiO_2 ratio to 0.78 for CS7P60. According to Rankin classification of hydraulicity, a $CaO/SiO_2 < 0.5$ is pozzolanic, 1–1.5 is latent hydraulic, and > 2 is hydraulic. The CaO/SiO_2 ratios of CS7 materials fall between 0.5 and 1, thus, it can be characterized as pozzolanic/latent hydraulic SCMs.

The high CaO/SiO_2 ratios of CS1, CS2, CS4, CS5, and CS6 indicate their potential to exhibit hydraulic reactivity – a critical property for cementitious materials. While CS3 and CS7 materials have a CaO/SiO_2 ratio that suggests some hydraulic potential, it is lower than that of the hydraulic category. Previous studies have shown that the slower reactivity of materials may be due to their lower CaO/SiO_2 ratio or the presence of certain mineral phases that influence reactivity. Thus, the same could be said about the materials being studied.

The latent hydraulic / hydraulic classifications of the CS suggest that their reactivity depends on specific environmental conditions

Table 4
Density and characteristic particle sizes of CS.

Material	Density (g/cm^3)	Particle Size (μm)			Laser Diffraction Specific Surface Area (m^2/kg)
		D_{10}	D_{50}	D_{90}	
CS1P0	2.29	13.6	118	683	158.3
CS1P30	2.39	4.82	31.1	401	445.1
CS1P60	2.49	3.65	24.9	257	580.7
CS2P0	1.86	10.8	112	901	195.6
CS2P30	2.09	5.22	24.2	551	451.1
CS2P60	2.1	4.26	33.9	427	527.4
CS3P0	2.58	5.85	42.8	350	384.4
CS3P30	2.59	4.51	39.9	307	460.1
CS3P60	2.6	3.68	34.8	318	592.3
CS4P0	1.63	10.6	108	571	217.1
CS4P30	1.83	5.03	32	149	440.5
CS4P60	2.01	3.12	23.4	152	715.2
CS5P0	2.5	11.7	161	706	177.1
CS5P30	2.52	9.67	189	607	200.5
CS5P60	2.59	12.4	210	503	170
CS6P0	2.57	7.96	76	457	305.5
CS6P30	2.64	5.82	68.4	368	384.3
CS6P60	2.69	4.92	57	321	439
CS7P0	2.51	6.73	37.2	208	342.7
CS7P30	2.53	4.87	26	86.4	471.3
CS7P60	2.55	4.32	24.2	91.5	533

or processing. The lower CaO/SiO_2 ratio of CS7 suggests that CS7 is primarily pozzolanic, and its reactivity is based on its ability to react with the $Ca(OH)_2$ produced during cement hydration. However, its pozzolanic/latent hydraulic classification suggests that CS7 may exhibit latent hydraulic behaviour in addition to pozzolanic properties.

The hydraulic characteristics concur with the findings of Vaičiukynienė *et al.* [20] and Jadhav *et al.* [21]. This characterization is

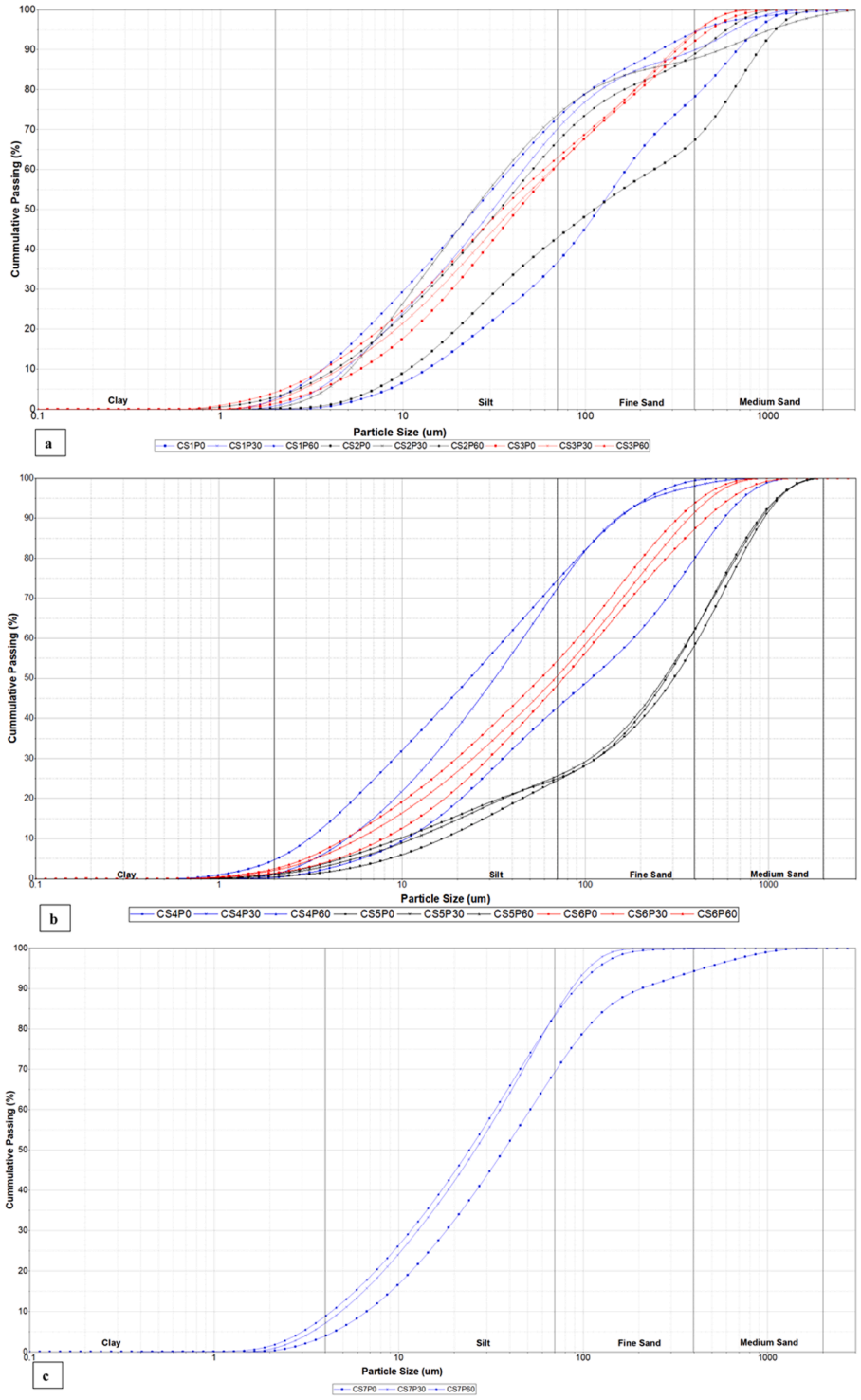

Fig. 2. PSD concerning the cumulative passing of a) CS from drilling and sawing operations, b) CS from the washing of concrete trucks and c) C7 stored for 2 years.

consistent with the pozzolanic class defined by ASTM C618 [13] as shown in Fig. 1. Though the chemical composition highlights the potential contribution and reactivity of CS, the mineralogical results, particularly the presence of amorphous phases in CS, are considered more significant indicators of its hydraulic properties and reactivity.

3.2. Physical properties

3.2.1. Particle density

The particle density values obtained, as shown in Table 4, range from 1.63 g/cm^3 to 2.69 g/cm^3 . This variation can be attributed to differences in the materials' composition and characteristics. The presence of different constituents, including sand, hydrated cement products, and any unhydrated cement particles, significantly influences CS's density. For instance, an increased sand content tends to raise the overall density of the material, approaching the density of sand, which is around 2.6 g/cm^3 . Conversely, the formation of CSH, a primary product of cement hydration, results in a lower density than sand, as CSH typically has a density of around 2.2 g/cm^3 . Unhydrated cement particles would also contribute to a higher density, as the density of cement ranges from 2.93 to 3.15 g/cm^3 .

CS2 exhibits a lower density of 1.86 g/cm^3 , suggesting a higher proportion of hydrated cement fines and lower sand content. This is supported by the PSD, which lacks medium sand and consists of finer particles. Additionally, the high amorphous phase content detected in CS2 (discussed later in XRD analysis) further supports the presence of hydrated products, contributing to its lower density. Similarly, CS4 exhibits the lowest density of 1.63 g/cm^3 among all CS, which can be attributed to a substantial proportion of binder minerals and minimal sand content. Its PSD and high surface area indicate finer particle composition with a significant amount of hydrated products.

On the other hand, materials like CS6, with a density of 2.69 g/cm^3 , exhibit a higher density closer to that of sand, indicating a greater sand content and possibly less hydrated products. The other samples' relatively narrow range of densities (2.3–2.7 g/cm^3) reflects a balanced composition of sand, hydrated cement products, and unhydrated cement particles.

The process of grinding and pulverization also plays a crucial role in the density variations observed. Grinding breaks down larger and agglomerated particles into smaller ones, enhancing packing efficiency and increasing particle density. This can be seen in the slight increases in density observed with more extensive pulverization. Additionally, it is important to consider the presence of intra-particle pores. Since the density of some samples increases quite drastically when the sample is ground/pulverized, it is likely that air-filled pores lower the density. For example, CS4's density increases from 1.6 to 2.0 g/cm^3 after grinding for 60 minutes, indicating that the density of the pulverized sample is more representative of the actual material.

3.2.2. Particle size distribution

The PSD of all CS samples is presented in Table 4. The specific surface area, determined through laser diffraction, increases with more extensive pulverization. This indicates that agglomerated particles are broken down into smaller particles, enhancing the reactivity of CS with water and other chemical compounds in the concrete mixture [23]. This increased reactivity is crucial for the pozzolanic or hydraulic reactions that SCMs undergo to contribute to the strength and durability of the concrete. The determined density of CS aligns with values reported in the literature [24].

The wide range of densities observed in the CS is due to the varying proportions of sand, hydrated cement products, unhydrated cement particles, and the effects of grinding and pulverization. Each factor contributes uniquely to the overall density, leading to the variations noted in the analysis.

Fig. 2 shows that most CS contain 35–50 % particles finer than 100 μm, with nearly identical PSD for these fractions across all CS.

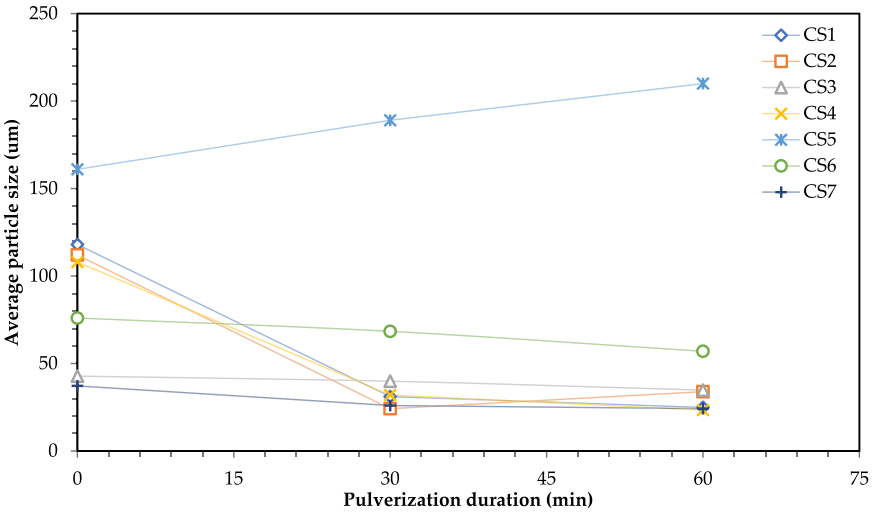

Fig. 3. Influence of pulverizing on the average particle size D50 of CSs.

The D90 values reveal a wide range of coarser particles in unpulverized CS, with CS2P0 exhibiting the most significant volume distribution. This observation aligns with the findings by Audo *et al.* [24] who, reported that half of the CS particles were smaller than 100 μm.

A noticeable difference in PSD and fineness is observed when comparing the majority of CS results, ranging from 30 to 60 minutes of pulverizing. After 30 minutes, D_{50} values ranged from 24.2 μm to 68.4 μm, and D_{10} values from 4.51 μm to 9.67 μm. After

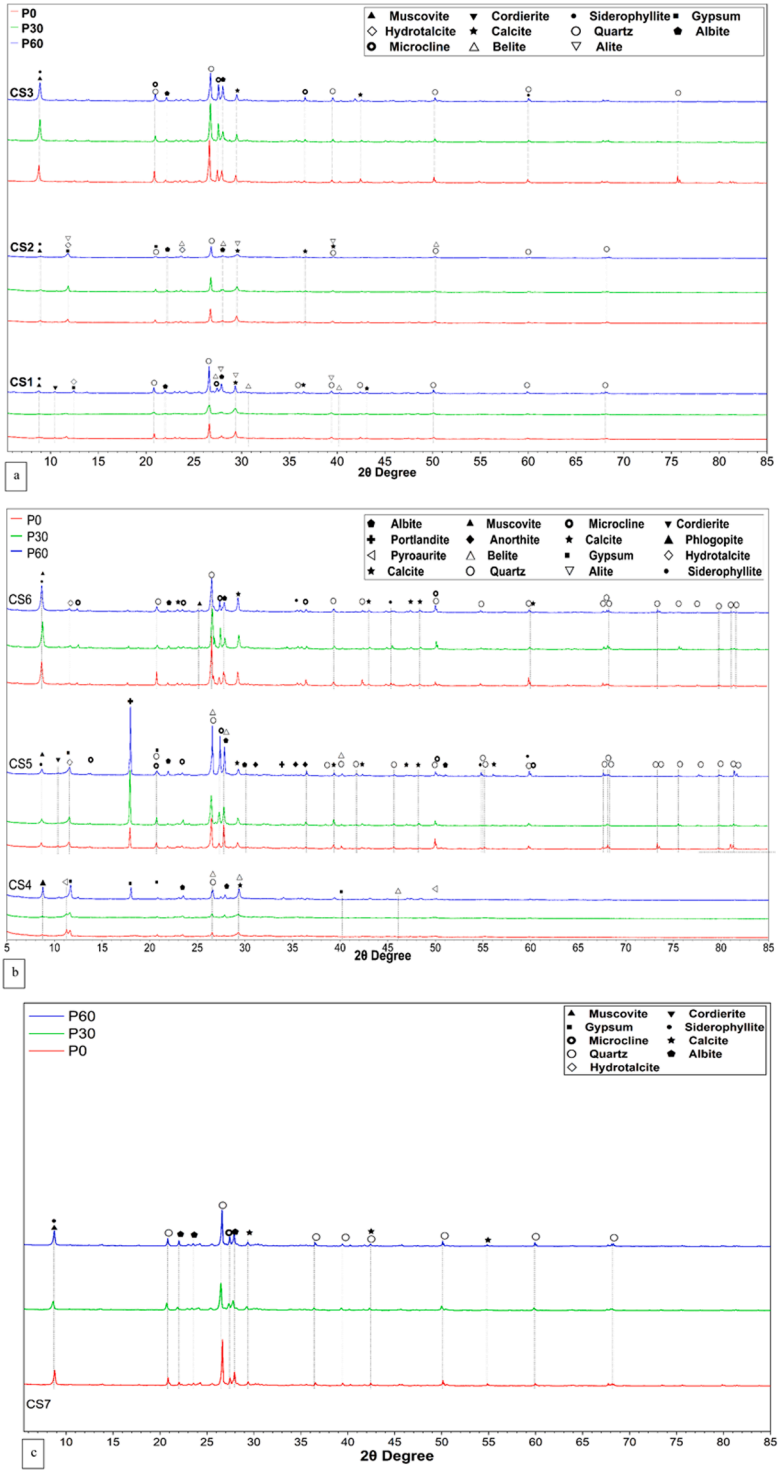

Fig. 4. XRD patterns of a) CS from drilling and sawing operations, b) CS from the washing of concrete trucks and c) C7 stored for 2 years.

60 minutes, D_{50} values were smaller, ranging from 23.4 μm to 57 μm, and D_{10} values from 3.12 μm to 4.92 μm. Fig. 3 highlights the influence of pulverizing on the average particle size D_{50} of CS. This indicates that extended pulverizing reduces particle size, though the reduction rate diminishes over time due to factors like re-agglomeration and increased resistance to size reduction.

Ready-mix plant CS samples exhibited a 10–70.37 % reduction in particle size after 30 minutes of pulverizing, while the drilling/sawing CS showed a 6.78–78.39 % reduction. CS1 experienced the most significant size reduction, likely due to its larger initial particles, whereas CS5 had the lowest size reduction, potentially due to a higher proportion of coarse sand. After 60 minutes of pulverizing, particle size decreased by 6.9–26.88 % compared to 30 minutes. The initial rapid size reduction slows as particles become smaller and more resistant to further reduction. Thus, limiting pulverizing to 30 minutes is advisable to minimize energy consumption while achieving similar fineness.

According to the USDA soil classification, CS1, CS4, CS5, and CS6 have a significant proportion of particles within the fine and medium sand ranges, indicating a predominance of aggregate residues. In contrast, CS2, CS3, and CS7 contain fewer particles within these ranges. Hard minerals such as quartz and feldspar, found in the medium and fine sand fractions, contribute to the smaller decrease in average particle size after extended pulverizing.

3.3. Mineralogical composition

The minerals/phases associated with the binder in this study include alite, gypsum, belite, and portlandite. Fig. 4 illustrates the XRD diffractograms of all CS samples, revealing similar peaks with varying proportions. The specific peaks of CS indicate the presence of several significant phases.

The typical sand-derived minerals identified include quartz (SiO_2), calcite ($CaCO_3$), albite ($NaAlSi_3O_8$), microcline ($KAlSi_3O_8$), anorthite ($CaAl_2Si_2O_8$), and cordierite ($2MgO.2Al_2O_3.5SiO_2$). Typical cement-derived minerals include calcite ($CaCO_3$), gypsum ($CaSO_4{\cdot}2H_2O$), portlandite ($Ca(OH)_2$), hydrotalcite ($Mg_6Al_2(CO_3)(OH)_{16}.4(H_2O)$), and conglomerations of CSH, anorthite ($CaAl_2Si_2O_8$), and cordierite ($2MgO.2Al_2O_3.5SiO_2$).

$CaCO_3$ may arise from the carbonation of $Ca(OH)_2$, a cement hydration product, while $CaSO_4{\cdot}2H_2O$ can form a byproduct of cement hydration reactions. $Ca(OH)_2$, $CaAl_2Si_2O_8$ and $2MgO.2Al_2O_3.5SiO_2$ represent various compounds formed during the cement hydration process or as impurities in raw materials. Some CS exhibited peaks for gypsum, as well as anhydrous calcium silicates. The presence of anhydrous calcium silicates, specifically belite (C_2S) and alite (C_3S), shows a potential residual hydraulic activity, while no ettringite was identified.

The high mineralogical content of quartz, feldspar minerals, and $KAlSi_3O_8$ (including albite, anorthite, microcline, and sanidine), as well as mica minerals such as muscovite, phlogopite ($KMg_3AlSi_3O_{10}(F, OH)_2$), and siderophyllite ($KFe^{2+}{}_2Al(Al_2Si_2)O_{10}(F, OH)_2$), can be attributed to the particles accumulated from fine aggregates.

From the XRD analysis, it is evident that the aggregate source of the concrete plant significantly influences the mineralogical composition of the CS, with variations observed in the quantities of quartz, feldspar, and mica minerals among the different CS sources. While calcite has been observed to enhance properties by accelerating the hydration process through a phenomenon known as the nucleation effect, it has also been reported that an excessive presence of calcite can lead to a phenomenon known as the dilution effect. This excessive presence, instead of supporting reactivity, may result in a concurrent deterioration in cementitious composites' mechanical properties and long-term durability. Therefore, the dual role of calcite in both supporting reactivity and causing dilution should be carefully considered in the overall assessment of its impact on cementitious materials. These findings are consistent with previous literature on CS [24], where quartz, calcite, and calcium silicates were reportedly the significant minerals detected. The mineralogical composition of CS is presented in Table 5.

Furthermore, a change in peak intensity can be observed for samples after pulverization; this is often due to the variation in the orientation of crystalline grains within the sample. The peaks also become broader after pulverization; this could be due to de-agglomeration once the CS was pulverized, thus causing a distribution of crystal sizes and orientations [25,26]. Additionally, when two or more minerals have similar crystal structures and lattice parameters, peak overlap may occur; however, when the material is pulverized, it could cause the crystal grains of both minerals to become smaller or more randomly oriented, leading to reduced peak intensity [27,28]. Variability in both sample characteristics and the inherent randomness in analytical processes can lead to non-identical results when the same sample is analyzed multiple times.

As mentioned earlier, approximately 40 %, 75 % and 50 % of the particles of CS4, CS5, and CS6, respectively, lay between fine and medium sand limitations, thus suggesting that most of the material contains a higher content of aggregates than binder minerals, with the help of XRD, this can be observed as shown in Fig. 5.

It can be observed that with the pulverization of CS, the content of minerals from aggregates and binders suggests that the amorphous content varies across the CS, ranging from approximately 2.29–28.47 %. The amorphous content in a material typically indicates the presence of non-crystalline or disordered structures within the material. While the CS may include unhydrated particles, which are crystalline components, it also comprises amorphous content, which can be attributed to the CSH gels and fly ash residue, which may not have been entirely consumed during the pozzolanic reaction. The unhydrated particles, especially if the particles contain pozzolanic properties, will react with water and contribute to the formation of additional hydrated products, potentially leading to additional strength development. The amorphous content is often of interest in cementitious materials because amorphous materials tend to be more reactive than crystalline ones.

The amorphous content in CS was determined using XRD and the internal standard method with calcium fluoride as the standard. The XRD patterns were obtained for each sample, and the crystalline phases were identified and quantified using Rietveld refinement. The amorphous content was then calculated by comparing the diffraction intensities of the crystalline phases with the known amount

Table 5
Mineralogical composition of all the CS.

Material	Amorphous	Alite	Calcite	Cordierite	Feldspar Group	Gypsum	Hydrotalcite Group	Belite	Mica Group	Portlandite	Pyrochroite	Quartz
CS1P0	5.21	22.27	21.71	0.85	13.46	7.11	0	0.95	2.16	0	0	24.27
CS1P30	13.38	22.95	19.84	1.04	10.49	5.37	0	0.78	2.43	0	0	22.26
CS1P60	7.08	13.09	15.61	2.51	27.32	1.21	0	0.47	2.05	0	0	29.55
CS2P0	8.2	20.11	20.56	1.29	12.85	7.9	0	0.64	2.85	0	0	22.13
CS2P30	8	22.63	17.85	1.38	12.68	8.28	0	0.46	2.47	0	0	21.16
CS2P60	12.83	17.7	13.6	0.95	7.4	8.36	0	1.04	1.75	0	0	16.99
CS3P0	8	0	8.28	1.56	36.14	1.01	0	0.46	2.39	0	0	36.89
CS3P30	5.73	0	8.48	1.41	39.49	0.47	0	0.09	11.68	0	0	31.39
CS3P60	4.63	0	9.54	1.62	39.38	1.23	0	0.76	12.2	0	0	28.89
CS4P0	12.83	0	15.95	3.85	19.08	14.3	0.17	12.29	6.09	3.57	0.43	9.76
CS4P30	28.47	2.65	10.08	1.28	11.85	15.88	0.5	21.17	0.64	0	0.57	5.15
CS4P60	11.35	0	16.4	3.9	19.14	14.44	0.19	12.68	6.11	3.63	0.1	10.16
CS5P0	8.92	0	10.11	3.19	28.98	0.91	0.18	8.47	1.36	2.19	0	32.97
CS5P30	4.23	0	11.01	2.59	35.05	0.58	0.1	7.66	2.68	2.68	0	30.93
CS5P60	3.08	0	7.17	12.89	33.74	1.64	0.19	3.97	2.41	2.13	0.1	31.21
CS6P0	2.29	0	17	0.98	24.72	0.97	0	0.88	13.97	0	0	38.2
CS6P30	3.88	0.87	16.53	1.73	30.07	0.29	0	0.96	10	0	0	34.7
CS6P60	10.77	0	16.14	1.7	26.86	1.07	0	0.62	13.19	0	0	28.73
CS7P0	4.4	0.67	6.21	1.72	39.97	0.86	0	0.76	5.059	0	0	39.67
CS7P30	4.8	0.57	7.17	1.43	42.54	0.38	0	0.76	4.96	0	0	37.09
CS7P60	7.08	0.27	7.46	1.7	41.62	0.97	0	0.633	6.36	1.43	0	35.6

Note: Feldspar group is the sum of albite, anorthite, microcline and sanidine
Hydrotalcite group is the sum of hydrotalcite and pyroaurite.
Mica group is the sum of muscovite and siderophyllite.

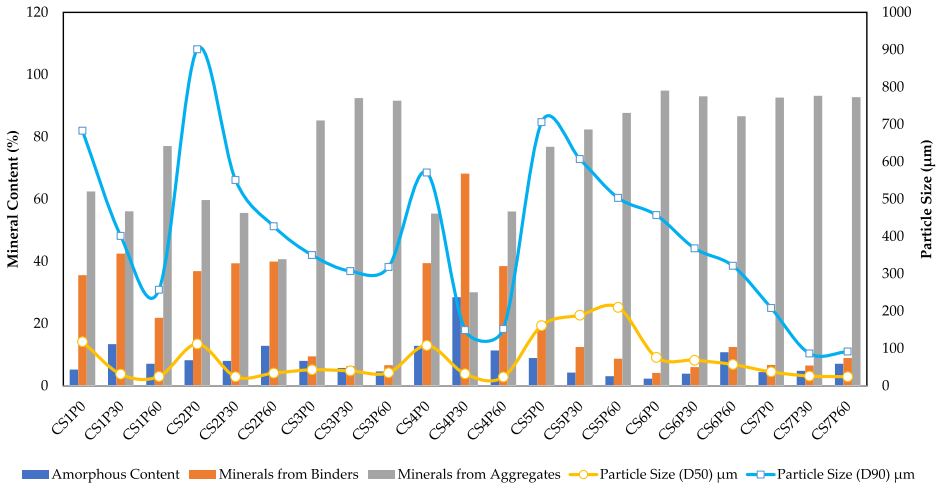

Fig. 5. Comparison of minerals from binders and aggregates with the particle size analysis.

of calcium fluoride, allowing for the determination the proportion of non-crystalline material.

The amorphous content in CS primarily arises from CSH, which forms during the hydration of cement and unreacted particles. Some amorphous silica may also be present due to carbonation, where CO_2 reacts with $Ca(OH)_2$ to form calcium carbonate and amorphous silica. Amorphous silica and unreacted fly ash exhibit pozzolanic properties, reacting with $Ca(OH)_2$ to form additional CSH and other hydrates, contributing to the material's strength and performance.

The D_{50} values range from approximately 23.4 µm to 210 µm, while D_{90} values range from 86.4 µm to 901 µm. These values reflect the PSD, with some samples having finer particles and others having coarser particles. The high amorphous content observed in CS4P30, measured at 28 %, cannot be solely attributed to amorphous silica, as XRF analysis indicates only 11 % SiO_2. The XRD results reveal a diverse array of crystalline phases, including alite (2.65 %), calcite (10.08 %), feldspar (11.85 %), gypsum (15.88 %), and belite (21.17 %), which can exist in amorphous forms under certain conditions.

The particle density of the CS4, approximately 1.63 g/cm^3 for unpulverized and 2.01 g/cm^3 for 60 minutes pulverized, may suggest the presence of lighter, potentially amorphous phases. The low SiO_2 content (~8.5–12 %) combined with the high content of CaO (~60–62 %) could indicate the formation of calcium-based compounds that contribute to these phases. The presence of amorphous silica, if present, might also be linked to the observed low density of CS4, as amorphous silica generally exhibits a lower density than its crystalline counterpart.

3.4. Microstructure and elemental analysis

The SEM with EDS analysis was conducted on CS3P0, CS3P30, CS4P0, CS4P30 and CS7P30, which can be seen in Fig. 6 and ANNEX I.

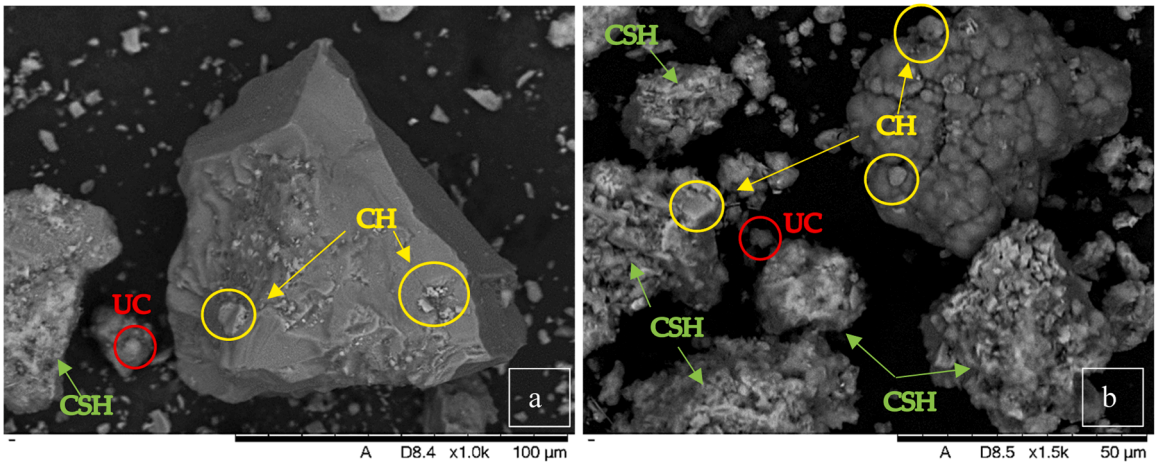

Fig. 6. SEM images at 1000X magnification of (a) CS3P30 and (b) CS4P30 Note: CSH = calcium silicate hydrate, CH = calcium hydroxide and UC = unreacted cement.

Fig. 6(a), an SEM image of precast CS (CS3P30), exhibits visibly dominant are hydration products such as CSH, ettringite, and CH, along with traces of unreacted cement particles. The CSH is primarily observed as amorphous, gel-like structures with irregular, dense textures, indicative of its role as the primary binding phase in hydrated cementitious systems. Plate-like or layered crystals, typical of CH, are also identified, reflecting its crystalline nature and contribution to the alkalinity of the cement matrix. In addition to these hydration products, some spherical and dense particles are visible, likely representing unreacted cement grains or filler materials, which appear with sharper edges and higher contrast compared to the hydration phases.

Whereas, Fig. 6(b), an SEM image of readymix CS (CS4P30), exhibits a large amount of irregular and flake-like structures, which may correspond to CSH, a primary hydration product forming a dense, amorphous gel-like matrix. As observed from XRD analysis, CS4P30 contains 28.47 % amorphous content. Thus, the large presence of CSH in the SEM image verifies that the amorphous content is correct. Additionally, some areas appear rough and uneven, with evidence of fragmented or layered features, likely associated with CH. A large particle is also clearly visible which seems to contain cracks and suggesting it may crumble under further mechanical action.

From the SEM images as shown in ANNEX I, CS4P0 appears predominantly coarse, with a particle size ranging between 10 – 20 μm, and with larger clusters exceeding 30 μm. The particles exhibit an irregular and angular shape, validating that CS4P0 is either pulverized or incomplete grinding. In contrast, CS4P30 showed finer particles, mostly 1 – 5 μm particle size along with some agglomerates forming secondary structures. Compared to CS4P0, the particles are more rounded and uneven in CS4P30, suggesting improved surface area, due to pulverization. CS3P0 exhibits a coarser structure like CS4P0, with particle size ranging approximately from 10 to 25 μm. The particles are irregular in shape with a higher proportion being flaky or plate-like, which could potentially indicate the presence of siliceous phases. As for CS3P30, the pulverization allowed it to gain finer particles like CS4P30 exhibited, while the particles had smoother but rounded shape. CS7P30 revealed that there were some traces of submicron particles, the shape of particles was mostly smooth and compact, with minimal angularity. Age appeared to have stabilized the particle surface through secondary reactions, likely forming carbonate phases.

From EDS images in ANNEX II, it can be observed that calcium (Ca) dominates the spectrum, with silica (Si) relatively lower than Ca, and other components with minimum intensity. This suggests that CS4P0 contains lime-rich phases with limited potential pozzolanic activity. Similar EDS results for CS4P30 can be observed, with Ca remaining the dominant element being highlighted, while the intensity of other elements varies but still is minimal. For CS3P0, the EDS has both Ca and Si dominating the spectrum, thus indicating that there is a balance of siliceous and calcareous phases. It can also be observed that other elements such as K are also visible, reflecting the alkali-rich nature of precast CS. After 30 minutes, not much has changed in the EDS of CS3P30, Si and Ca still being the dominant elements to be visible. The pulverization may have increased the exposure of calcareous phases slightly more after pulverization, thus indicating that by pulverizing CS4, reactivity may increase with minimal reduction in siliceous content. As for CS7P30, it is quite similar to CS4P30, with Si and Ca being the dominant elements detected by EDS, it could also indicate of ongoing reactions as well as stabilization of siliceous phases, which could potentially improve long-term durability aspects. Comparatively the EDS showed the precast CS exhibited higher siliceous and alkali content, as evidenced by the increased feldspar and quartz phases as shown in Table 5, making them more suitable for potential pozzolanic reactions. Likewise, the ready-mix CS are shown to be lime-rich, containing higher alite, belite and portlandite phases as observed in Table 5, making them ideal for hydraulic reactions and early strength development. Though, CS7P30 is from a similar source as CS3, but it was stored in closed environment for 2 years, shows that aging led to stabilized siliceous and carbonate phases.

4. Conclusion

The pursuit of reducing the environmental impact of cement production has spurred research into substantial clinker replacement, prompting innovative approaches to harness the potential of emerging SCMs. By employing a screening approach to identify promising materials for substituting cement, we can achieve more substantial replacements and expedite the adoption of new SCMs.

This study utilized various existing non-destructive characterization methods (density, chemical composition, mineralogical composition, particle size analysis, and SEM-EDS) to provide a systematic approach to assessing CS as a potential SCMs. The findings revealed that:

1. All CS samples satisfied the MgO, P_2O_5, and SO_3 limits of EN 450–1. Most CS exhibited hydraulic characteristics based on Rankin's classification, while CS7 satisfied ASTM C618's Class C pozzolan requirements. However, when applying Rankin's classification to materials partly constituted of sand, caution must be taken.
2. High Fe_2O_3 levels in CS1, CS2, CS3, and CS7 likely result from manufacturing processes, raw material composition (sand and paste), and potential contamination from steel fibres or fragments during cutting and drilling.
3. 30 minutes pulverizing ready-mix and precast CS, reduced particle size by 10–70.37 % and 6.78–78.39 %, respectively. An additional 30 minutes of pulverization only added 6.9–26.88 % more reduction. The most significant reduction occurs in the first 30 minutes, suggesting this duration is optimal to minimize energy use while achieving the desired fineness.
4. XRD analysis revealed that most CS samples have an average amorphous content of 8.3 %, ranging from 2.29 % to 28.47 %. CS4 exhibited significantly higher amorphous content, which cannot be solely attributed to amorphous silica (11 % SiO_2 by XRF). Additional components such as alite, calcite, cordierite, feldspar, gypsum, hydrotalcite, belite, mica, portlandite, pyrochroite, and quartz contribute to this elevated content. These findings suggest that CS4's complex composition, beyond silica alone, is responsible for its high amorphous phase, indicating a need for further analysis to fully understand it.

5. CS is composed of fine aggregates and hydrated/carbonated cement residuals. Density varies with sand (up to 2.6 g/cm^3), CSH (~2.2 g/cm^3), and unhydrated cement, and is affected by intra-particle pores. Grinding reduces these pores, making density measurements more accurate. For instance, CS4's density increased from 1.6 to 2 g/cm^3 after 60 minutes of grinding, reflecting reduced porosity.
6. Rapid analytical methods revealed that CS7, stored in a closed environment for two years, exhibited an increase in pozzolanic oxides compared to CS3, suggesting that aging may influence the chemical and mineralogical properties of concrete sludge. However, these differences could also be attributed to variability in production methods or raw materials rather than solely the effect of aging.
7. Though the material properties vary for each CS, however, the CS can be generalized into two SCMs based on their operation: precast CS, characterized by siliceous and alkali-rich properties, and ready-mix CS, which is lime-rich and exhibits hydraulic properties.
8. SEM-EDS analysis verified pulverization of CS lead to finer, rounded particles while unpulverized CS being coarser and angular shaped. EDS identified Ca and Si as dominant, with precast CS being siliceous and alkali-rich for pozzolanic reactivity, while ready-mix CS was lime-rich, favoring hydraulic reactions.

4.1. Recommendations/future works

Based on the current study, it is recommended that future research be conducted to build on this preliminary material characterization work by incorporating the CS as a partial cement replacement in the preparation of concrete elements. The next step involves assessing the fresh-state, mechanical and durability properties of concrete incorporating CS to determine whether the promising material characteristics observed in this study translate into practical performance as SCMs.

Additionally, future work will focus on optimizing the proportioning of CS as a cement replacement, exploring its interactions with other components in the mix, and evaluating long-term properties. Further investigations may also consider the influence of varying sludge treatment methods (e.g., pulverization levels) and curing conditions on performance outcomes. By extending this research, we aim to provide a comprehensive understanding of the potential of CS as an eco-friendly and effective SCM, while addressing any challenges associated with its practical application.

Funding

The outcome has been achieved with the financial support of the Circulus Project Nr. 299322 funded by the Norwegian Research Council.

CRediT authorship contribution statement

Jhatial Ashfaque Ahmed: Writing – review & editing, Writing – original draft, Visualization, Validation, Methodology, Investigation, Formal analysis, Data curation, Conceptualization. **Novakova Iveta:** Writing – review & editing, Writing – original draft, Validation, Supervision, Funding acquisition, Conceptualization. **Gjerløw Eirik:** Writing – review & editing, Writing – original draft, Visualization, Validation, Supervision, Formal analysis. **Engelsen Christian John:** Writing – review & editing, Visualization, Validation, Formal analysis.

Declaration of Competing Interest

The authors declare the following financial interests/personal relationships which may be considered as potential competing interests: Iveta Novakova reports financial support was provided by Research Council of Norway. If there are other authors, they declare that they have no known competing financial interests or personal relationships that could have appeared to influence the work reported in this paper.

Appendix A. Supporting information

Supplementary data associated with this article can be found in the online version at doi:10.1016/j.cscm.2025.e04319.

Data Availability

All the data used in the study has been shared within the research paper.

References

[1] A. Naqi, J. Jang, Recent progress in green cement technology utilizing low-carbon emission fuels and raw materials: a review, Sustainability 11 (2) (2019) 537, https://doi.org/10.3390/su11020537.
[2] E. Benhelal, E. Shamsaei, M.I. Rashid, Challenges against CO2 abatement strategies in cement industry: a review, J. Environ. Sci. 104 (2021) 84–101, https://doi.org/10.1016/j.jes.2020.11.020.
[3] A.A. Jhatial, I. Nováková, E. Gjerløw, A review on emerging cementitious materials, reactivity evaluation and treatment methods, Buildings 13 (2) (2023) 526, https://doi.org/10.3390/buildings13020526.
[4] N.Z. Roadmap, "A Global Pathway to keep the 1.5° C Goal in Reach," International Energy Agency, 2023.
[5] J. Nilimaa, Smart materials and technologies for sustainable concrete construction, Dev. Built Environ. 15 (2023) 100177, https://doi.org/10.1016/j.dibe.2023.100177.
[6] I. Nováková, et al., Investigating the influence of oil shale ash and basalt composite fibres on the interfacial transition zone in concrete, Buildings 14 (7) (2024) 1952, https://doi.org/10.3390/buildings14071952.
[7] M. Keppert, V. Davidová, B. Doušová, L. Scheinherrová, P. Reiterman, Recycling of fresh concrete slurry waste as supplementary cementing material: characterization, application and leaching of selected elements, Constr. Build. Mater. 300 (2021) 124061, https://doi.org/10.1016/j.conbuildmat.2021.124061.
[8] E. Pocius, D. Nagrockienė, I. Pundienė, The influence of concrete sludge from residual concrete on fresh and hardened cement paste properties, Materials 16 (6) (2023) 2531, https://doi.org/10.3390/ma16062531.
[9] M. Schneider, The cement industry on the way to a low-carbon future, Cem. Concr. Res 124 (2019) 105792, https://doi.org/10.1016/j.cemconres.2019.105792.
[10] EMRCO, "European Ready Mixed Concrete Organization, Ready-Mixed Concrete Industry Statistics: Year 2018," 2019. Accessed: Jul. 03, 2024. [Online]. Available: ⟨http://ermco.eu/new/wp-content/uploads/2020/08/ERMCO-Statistics-30.08.2019-R4-1.pdf⟩.
[11] L. de B.P. Vieira, A.D. de Figueiredo, Evaluation of concrete recycling system efficiency for ready-mix concrete plants, Waste Manag. 56 (2016) 337–351, https://doi.org/10.1016/j.wasman.2016.07.015.
[12] M.C.G. Juenger, R. Snellings, S.A. Bernal, Supplementary cementitious materials: new sources, characterization, and performance insights, Cem. Concr. Res 122 (2019) 257–273, https://doi.org/10.1016/j.cemconres.2019.05.008.
[13] ASTM C618-19, "Standard Specification for Coal Fly Ash and Raw or Calcined Natural Pozzolan for Use in Concrete, ASTM International, West Conshohocken, PA, 2019, ⟨www.astm.org⟩," 2019.
[14] University of Massachusetts, "Convert oxides to elements (and vice versa)."
[15] EN 1097-7, "Tests for mechanical and physical properties of aggregates - Part 7: Determination of the particle density of filler - Pyknometer method," 2022.
[16] P. Zhao, X. Liu, A.G. De La Torre, L. Lu, K. Sobolev, Assessment of the quantitative accuracy of Rietveld/XRD analysis of crystalline and amorphous phases in fly ash, Anal. Methods 9 (16) (2017) 2415–2424, https://doi.org/10.1039/C7AY00337D.
[17] I. Ismail, Arliyani, S. Fathmiyah, Mursal, Z. Jalil, H.P.S.A. Khalil, Effect of ball-milling time on chemical property of coconut shell powder, J. Phys. Conf. Ser. 1572 (1) (2020) 012021, https://doi.org/10.1088/1742-6596/1572/1/012021.
[18] EN 450-1, "Fly ash for concrete - Definition, specifications and conformity criteria," 2012.
[19] Y. Ye, et al., Effect of nano-magnesium oxide on the expansion performance and hydration process of cement-based materials, Materials 14 (13) (2021) 3766, https://doi.org/10.3390/ma14133766.
[20] D. Vaičiukynienė, et al., Synergistic effect of dry sludge from waste wash water of concrete plants and zeolitic by-product on the properties of ternary blended ordinary Portland cements, J. Clean. Prod. 244 (Jan. 2020) 118493, https://doi.org/10.1016/j.jclepro.2019.118493.
[21] P.J. Jadhav, N.A. Mohite, V.S. Kadam, and M.M. More, "Effect of concrete sludge from residual concrete on hardened cement paste properties."
[22] A. Sicakova, M. Kovac, Technological characterization of selected mineral additives, IOP Conf. Ser. Mater. Sci. Eng. 385 (Jul. 2018) 012048, https://doi.org/10.1088/1757-899X/385/1/012048.
[23] U.J. Alengaram, Valorization of industrial byproducts and wastes as sustainable construction materials. Handbook of Sustainable Concrete and Industrial Waste Management, Elsevier, 2022, pp. 23–43, https://doi.org/10.1016/B978-0-12-821730-6.00003-6.
[24] M. Audo, P.-Y. Mahieux, P. Turcry, Utilization of sludge from ready-mixed concrete plants as a substitute for limestone fillers, Constr. Build. Mater. 112 (2016) 790–799, https://doi.org/10.1016/j.conbuildmat.2016.02.044.
[25] L. Krishnaraj, P.T. Ravichandran, Investigation on grinding impact of fly ash particles and its characterization analysis in cement mortar composites, Ain Shams Eng. J. 10 (2) (2019) 267–274, https://doi.org/10.1016/j.asej.2019.02.001.
[26] S. Dĭkmen, Z. Dĭkmen, G. Yilmaz, S. Firat, Mechanical activation of fly ash: physical, mineralogical and morphological characterization of ground fly ashes, Eskişehir Tech. Univ. J. Sci. Technol. A - Appl. Sci. Eng. 20 (2019) 66–76, https://doi.org/10.18038/estubtda.637927.
[27] J.R. Deschamps, J.L. Flippen-Anderson, Crystallography. Encyclopedia of Physical Science and Technology, Elsevier, 2002, pp. 121–153, https://doi.org/10.1016/B0-12-227410-5/00160-5.
[28] P. Thakur, A. Thakur, Nanomaterials, their types and properties. Synthesis and Applications of Nanoparticles, Springer Nature Singapore, Singapore, 2022, pp. 19–44, https://doi.org/10.1007/978-981-16-6819-7_2.